

Article

Flower-like BiVO₄ Microspheres and Their Visible Light-Driven Photocatalytic Activity

Arini Nuran Zulkifili ¹, Akira Fujiki ² and Shinji Kimijima ^{2,*}

¹ Graduate School of Engineering, Shibaura Institute of Technology, Saitama 337-8570, Japan; na15101@shibaura-it.ac.jp

² Department of Machinery and Control Systems, Shibaura Institute of Technology, Saitama 337-8570, Japan; a-fujiki@sic.shibaura-it.ac.jp

* Correspondence: kimi@sic.shibaura-it.ac.jp; Tel.: +81-48-687-5124

Received: 13 November 2017; Accepted: 22 January 2018; Published: 31 January 2018

Abstract: A flower-like BiVO₄ microsphere photocatalyst was synthesized with a simple template-free homogeneous precipitation method at 60 °C for 24 h. The purpose of this study is to explore a low-cost, simple method of synthesizing the self-assembled 3D structure in order to enhance photocatalytic performance under visible light irradiation ($\lambda > 420$ nm). In this study, the morphology, structure, and photo-absorption of flower-like BiVO₄ microspheres were characterized, and the effects of photocatalysis were analyzed. The results indicate that the size of the flower-like microspheres was about 2 μm to 4 μm and they were composed of several nanosheets. The mechanism of hierarchical microsphere formation has been proposed as the Ostwald ripening process and the self-assembled process. The obtained samples were calcined under different temperatures (300 °C, 400 °C, 500 °C and 600 °C) to study the effects of calcination on the structure and on photocatalysis. The photocatalytic process was then evaluated by decolorization of methylene blue dye under visible-light irradiation.

Keywords: bismuth vanadate; low-cost method; methylene blue dye; microspheres; photocatalyst; visible light

1. Introduction

In recent years, photocatalysts have attracted much attention due to their wide range of applications, from generating hydrogen by splitting water to decomposing organic contaminants in wastewater [1]. In the decomposition of organic contaminants such as dyes in wastewater, the photocatalyst uses visible light or ultraviolet (UV) light as an irradiating source to mineralize the contaminants in order to produce the end products such as carbon dioxide and water. TiO₂ has been the subject of early study in photocatalytic materials. However, due to its wide band gap, it can only work under ultraviolet irradiation for photocatalytic activation, which leads to very low energy efficiency in utilizing solar light. This is because UV light is only utilizing 5% solar energy, a small fraction compared to visible light, which is 45% [2]. Therefore, research has been focused on finding a method or materials that can work efficiently under visible light irradiation.

Among the widely studied materials are bismuth-based photocatalysts, which have been proven to be suitable in the degradation of organic contaminants under visible light irradiation [3]. This is because bismuth compound such as Bi₂O₃, BiVO₄, NaBiO₃ has a band gap range less than 3.0 eV and is environmentally friendly. Various approaches in synthesizing BiVO₄ have been reported. A monoclinic BiVO₄ has successfully been prepared by solid state reaction (SSR) and by melting at a high temperature [4], whereas, a tetragonal BiVO₄ has been synthesized by a precipitation method at a room temperature [5]. In addition, a simple aqueous process in preparing both monoclinic and tetragonal phase was also reported [6]. In addition, the use of hydrothermal process in creating various

structural, morphologies and phase were also being reported. Since BiVO_4 can be prepared by using a simple method, it is one of the suitable candidates in the study of a low-cost synthesis method [7].

Besides that, nano-size photocatalytic materials have been proven to have a high degradation rate in degrading organic contaminants, due to their having a greater surface area, which provides more fine contact among catalyst particles and organic substrate, good dispersion, and abundant active sites. However, the recovery process becomes a drawback for this nano-size photocatalyst, since the powder-like nano-photocatalyst often suffers from deactivation, agglomeration, and difficulty settling for recycling after the initial run. This makes it hard to recycle the photocatalyst, and nonrecyclable photocatalytic materials will increase operating cost, which significantly limits their application in wastewater treatment. In most wastewater treatment, photocatalysts are suspended in aqueous solution. Separation of photocatalysts must be done by settling with the aid of gravity or mechanical centrifugation. Settling of ultrafine photocatalyst particles with the aid of gravity has been commonly observed to proceed very slowly.

Therefore, in this study, we developed a microstructure photocatalyst composed of nanosheets to enhance the process by using a simple, low-cost method that results in the formation of a flower-like bismuth vanadate microstructure that has a greater surface area, more stability, and higher efficiency in organic dye degradation under visible light irradiation. As for the dye contaminant, we chose methylene blue (MB) dye because it is a frequently used industrial dye. MB dye has the chemical structure of $\text{C}_{16}\text{H}_{18}\text{N}_3\text{S}^+\text{Cl}^-$ and is shown in Figure 1.

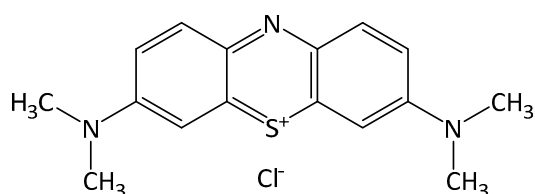


Figure 1. Structure of methylene blue dye.

2. Materials and Methods

Bismuth nitrate pentahydrate ($\text{Bi}(\text{NO}_3)_3 \cdot 5\text{H}_2\text{O}$) crystal and nitric acid (HNO_3) were purchased from Wako Pure Chemical Industries (Osaka, Japan). Sodium hydroxide (NaOH) granule was purchased from Kanto Chemical Co., Inc., (Tokyo, Japan) vanadium (III) acetylacetonate ($\text{C}_{10}\text{H}_{14}\text{O}_5\text{V}$) crystal from Strem Chemicals Inc., (Newburyport, MA, USA) and methylene blue dye powder from Waldeck GmbH & Co. KG (Münster, Germany). Ultrapure water was used in all experiments. All chemicals were analytical grade and used as received, without further purification.

Flowerlike BiVO_4 microspheres were synthesized by a simple template-free precipitation method at 60°C for 24 h. Then, 4.2 g of $\text{Bi}(\text{NO}_3)_3 \cdot 5\text{H}_2\text{O}$ and 0.27 g of $\text{C}_{10}\text{H}_{14}\text{O}_5\text{V}$ were dissolved in 100 mL of HNO_3 at a concentration of 4 mol L^{-1} . Ultrapure water was added until it reached a final volume of 500 mL. The solution was stirred until a clear light blue solution was formed. Then, the pH of the solution was adjusted to 12 by adding NaOH . The solution changes color from clear light blue to bluish precipitate and brownish precipitate, which indicates the change from acidic to neutral to alkaline state. The suspension was inserted into an oil bath at 60°C for 24 h without stirring. The resulting yellow precipitate was retrieved by centrifugation, and washed several times with distilled water and absolute ethanol. The yellow precipitate was then dried at 60°C for 24 h and was calcined at different temperatures (300°C , 400°C , 500°C and 600°C) for further study.

The samples were analyzed with an X-ray diffractometer (XRD; RINT 2000, Rigaku Corp., Tokyo, Japan) operated at 30 kV and 40 mA with $\text{Cu K}\alpha$ radiation ($\lambda = 1.54178\text{ \AA}$). Data were collected in the angular range of $2\theta = 15\text{--}80^\circ$. Field emission scanning electron microscopy images were obtained from a Hitachi FE-SEM SU8000 (Tokyo, Japan). UV-visible diffusion reflectance spectra were measured at room temperature with a JASCO V-7200 UV-Vis-NIR Spectrophotometer

(Jasco Products Company, Oklahoma City, OK, USA). The reflectance was then converted to absorbance by using the Kubelka–Munk method. The size of the particles was recorded by zeta potential and an Otsuka Electronics ELSZ-2000 particle analyzer (Otsuka Electronics Co., Ltd., Osaka, Japan) at room temperature, using ultrapure water as a solution. Further analysis was conducted with a Thermo Scientific Nicolet 4700 Fourier-transform infrared spectroscopy analyzer (Thermo Fisher Scientific, Waltham, MA, USA), a Horiba-Jovin Yvon T64000 micro Raman spectrometer (HORIBA Jobin Yvon IBH Ltd., Paris, France), and a JASCO FP8500 fluorescence spectrometer.

Photocatalysis evaluation test was conducted as follows: 4 mL of methylene blue solution at a concentration of 0.3 mg/100 mL was placed in a 100 mL Pyrex vessel. Then, 96 mL of ultrapure water was added to the aqueous solution. After that, 0.3 g of BiVO_4 powder was added for each experiment. The experiments were conducted under the presence of visible light ($\lambda > 400$ nm). The solution was magnetically stirred to ensure uniformity. The samples were then filtered by using a syringe membrane filter (Millex; Millipore Corp., Burlington, MA, USA) to remove the photocatalyst particles. Samples were taken from the solution every 30 min and placed inside a UV-Vis spectrophotometer cell in order to measure the maximum absorption of wavelength for the dye and the rate of degradation. The percentage of degradation was calculated by the formula $[1 - (C/C_0)] \times 100\%$, where C_0 is the initial concentration of the dye solution and C is the concentration of the dye at each 30-min interval.

3. Result and Discussion

3.1. Material Characterization

XRD was used to characterize the phase structure of the obtained samples. Figure 2 shows the XRD pattern of the BiVO_4 microspheres prepared for each calcination temperature. The XRD pattern at 400 °C indicates that the sample was mainly in the monoclinic phase, which exhibits high photocatalytic activity compared to other phases. In addition, a well-defined sharp peak can be seen after calcination at 300 °C. This indicates that the sample achieved a well-defined organizational structure, which leads to better photocatalytic activity.

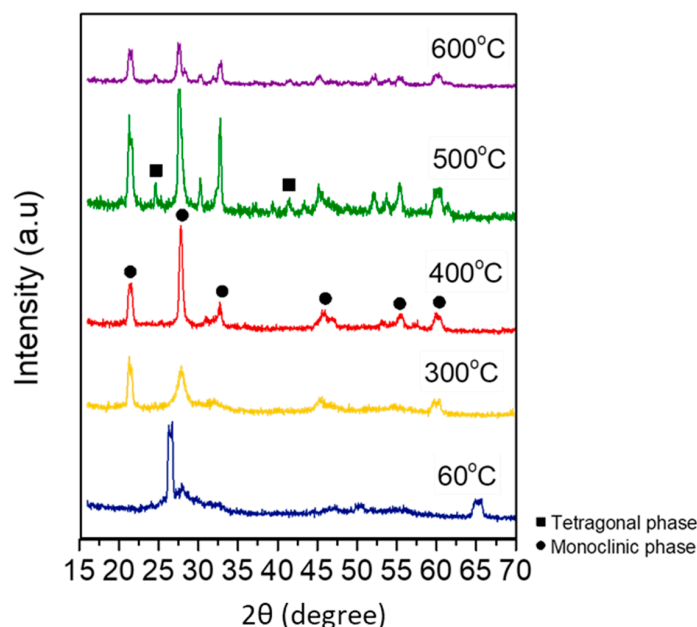


Figure 2. X-ray diffractometer (XRD) analysis for BiVO_4 microspheres under different calcination temperatures.

As shown in the scanning electron microscopy (SEM) observation images in Figure 3a–c, after calcination at 400 °C, the products formed were uniform. The SEM images of commercial BiVO₄ can be seen as bulky, and not much surface area is available.

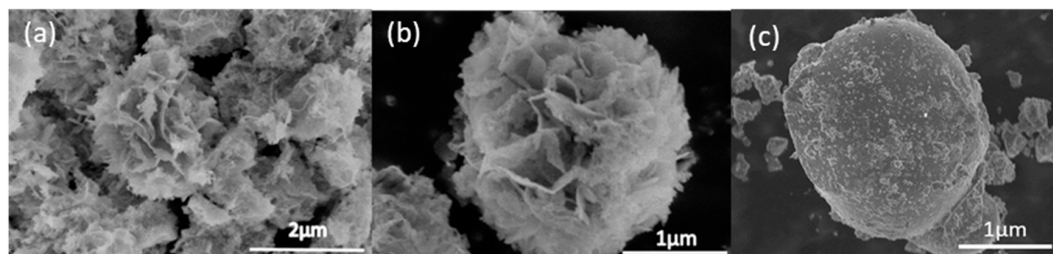


Figure 3. (a–c) Fourier-transform infrared spectroscopy images of flower-like BiVO₄; and (c) commercial BiVO₄.

At 500 °C (Figure 6), the mixture of flower-like structure and agglomerates started to form, while, at 600 °C, the particles started to form only agglomerates, and no flower-like structures were found.

To further study the morphologic structure, we observed the samples under high magnification SEM (Figure 4a,b), and the flower-like structures of the sample were composed of numerous nanosheets with a thickness of about 100 nm. The nanosheets intercrossed to form a flower-like microsphere via self-assembly and the Ostwald ripening process. These flower-like structures resulted in an increased surface area, which leads to better photocatalytic performance compared to commercial BiVO₄, which has a bulky structure and low surface area. Besides that, the large surface area provided by the flower-like structure can allow more rapid diffusion of the reactants and products during the reaction process. If we increased the pH of the synthesis condition to more than 12, the flower-like structure could not form, and only microspheres/microcubes would be observed.

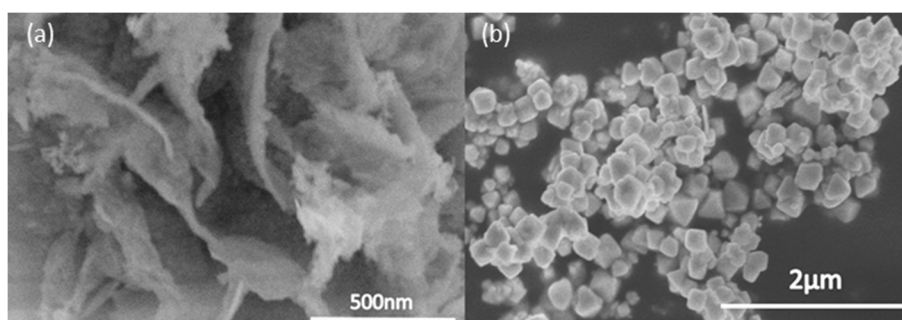


Figure 4. (a,b) High magnification of flower-like BiVO₄ and the results obtained under synthesis conditions of pH > 12.

We also proposed the formation mechanism of the flower-like BiVO₄ microspheres, as shown in Figure 5. A precipitation process occurred by the nucleation and growth of the second phase from a supersaturated solution. With a two-phase mixture composed of a dispersed second phase in a matrix, the mixture does not satisfy thermodynamic equilibrium. This is due to small particles with a higher surface ratio and a higher energy state leading to excess surface energy, which does not satisfy the requirement of minimum energy configuration. The total energy of this system can be decreased via an increase in the scale of the second phase, thus decreasing the total interfacial area. This will result in a continuous nucleation and growth process until a single precipitate particle forms, which introduces a new particle of a given size class, which, in this case, was the flower-like microsphere structure [8,9].

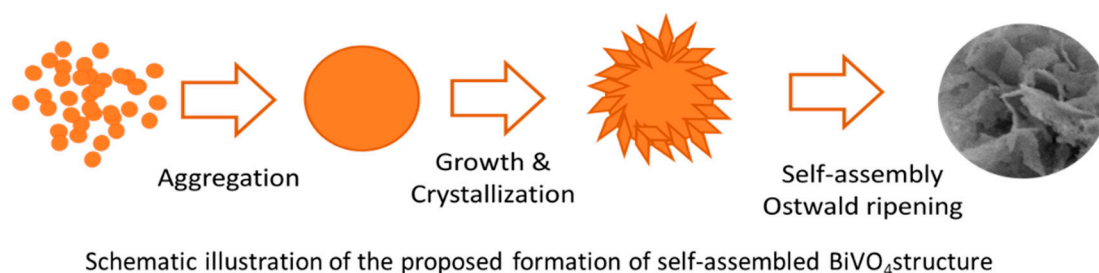


Figure 5. Schematic illustration of the proposed formation of flower-like BiVO₄ microsphere structure.

The mean particle size for the obtained samples was also studied using the zeta potential and particle analyzer. As shown in Figure 6, the smallest size was at 400 °C, which was 2566 nm with a slight error value. At 60 °C and 300 °C, the sample consisted of impurities, which led to a larger mean particle size. However, at 500 °C, the mean particle size was larger than at 400 °C, because a mixture of 3D microsphere structure and agglomerates started to form. The mean particle size became the largest, with a substantial error value at 60 °C due to most of the sample being made up of large agglomerates, contributing to poor photocatalytic performance.

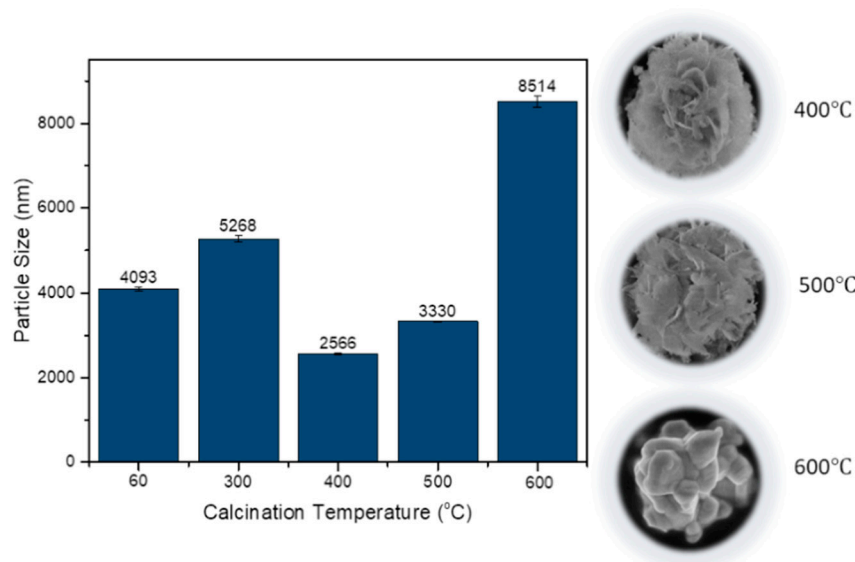


Figure 6. Particle size analysis of BiVO₄ microspheres under calcination temperatures of 60 °C, 300 °C, 400 °C, 500 °C and 600 °C.

3.2. Optical Properties

The UV-Visible optical absorption spectrum of BiVO₄ microspheres was measured and compared with commercial BiVO₄ and synthesized BiVO₄ microspheres, as shown in Figure 7. A broad absorption spectrum could be seen from 300 to 400 nm. At around 420 nm, an abrupt cutoff absorption edge was observed.

The absorption band contains a tail extending rightward until about 800 nm. This may be a result of crystal defects formation during the growth of the BiVO₄ microspheres. The band gap energy was determined by Kubelka–Munk derivation (Figure 7). The band gap of this photocatalyst is 2.60 eV, and it has yellowish colored powder. This shows that this photocatalyst can work efficiently under visible light irradiation. In addition, the presence of the monoclinic phase which has superior photocatalytic activity contributed to the enhancement of the photocatalytic character of this photocatalyst.

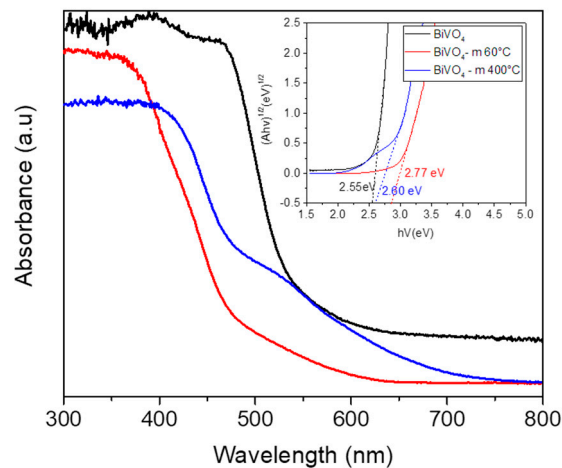


Figure 7. UV-Vis diffuse reflectance spectra of BiVO_4 microspheres.

Photoluminescence spectroscopy was studied at the excitation wavelength $\lambda_{\text{ex}} = 325$ nm. As shown in Figure 8, a strong peak can be seen at around 560 nm for both synthesized microspheres and commercial BiVO_4 . The strong emission at 560 nm corresponds to recombination of the hole formed from the hybrid orbitals of Bi 6s and O 2p and the electron generated from the V 3d orbitals. In addition, the emission bands of $\text{BiVO}_4\text{-m}$ have a blue shift compared to commercial BiVO_4 , which shows that it has a lower recombination rate.

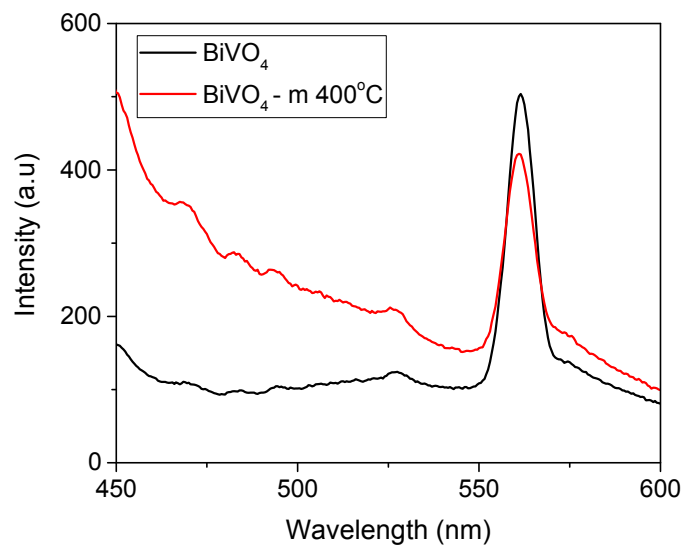


Figure 8. Photoluminescence spectra at the excitation wavelength $\lambda_{\text{ex}} = 325$ nm for BiVO_4 microspheres at 400 °C.

Raman spectroscopy was also investigated, as shown in Figure 9. The Raman bands at 313 cm^{-1} are the typical vibrations of BiVO_4 and can be assigned to the asymmetric and symmetric deformation modes of the VO_4^{3-} tetrahedron. It has been reported that there were two Raman bands, at 710 cm^{-1} and 805 cm^{-1} , which were attributed to the stretching modes of two different types of Vanadium–Oxygen bands in the Raman spectrum of BiVO_4 . However, only one band around 805 cm^{-1} was found in our case. The absence of a 710 cm^{-1} band might be attributed to the local structure of porous microspheres, which were composed of nanosheets. Additionally, the Raman band at 517 cm^{-1} indicates the characteristics of monoclinic scheelite BiVO_4 that made up these microsphere structures.

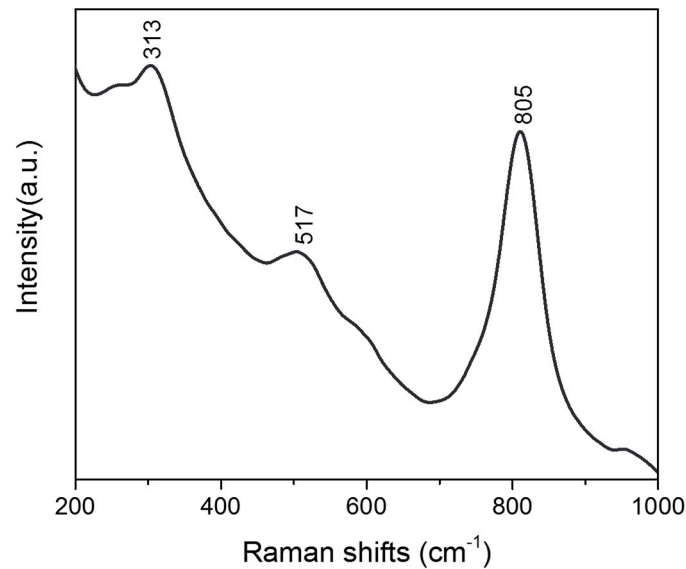


Figure 9. Raman analysis of BiVO_4 microspheres at $400\text{ }^\circ\text{C}$.

From the Fourier-transform infrared spectroscopy analysis we conducted (Figure 10), we can understand the bonding group presence in these BiVO_4 microspheres. At 1021 cm^{-1} , there is an unshared $\text{V}=\text{O}$ stretching vibration, followed by 833 cm^{-1} , which shows the presence of an asymmetric stretching vibration of the bound oxygen that is shared by two vanadium atoms ($\text{V}-\text{O}-\text{V}$). Furthermore, at 523 cm^{-1} , a symmetric stretching mode of the $\text{V}-\text{O}-\text{V}$ unit is present, and finally, at 3402 and 1627 cm^{-1} , it shows an $\text{O}-\text{H}$ stretching and bending vibration of the lattice water molecules [10].

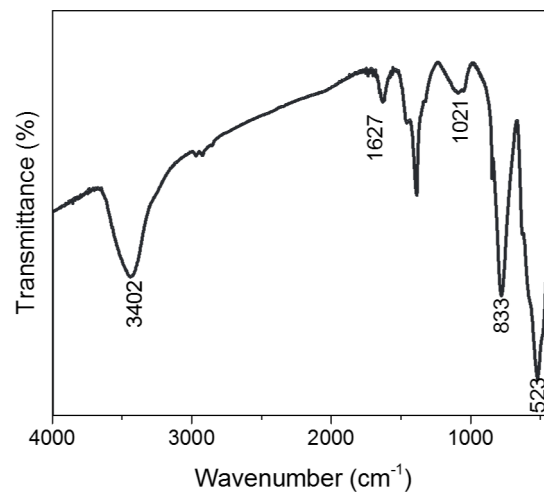


Figure 10. Fourier-transform infrared spectroscopy analysis of BiVO_4 microspheres at $400\text{ }^\circ\text{C}$.

We also conducted a zeta potential analysis to study the stability of this flower-like BiVO_4 in terms of the colloidal dispersion, as shown in Figure 11. This shows that it has high stability compared to commercial BiVO_4 , since it possesses a higher zeta potential value. When the potential is small, attractive forces can exceed this repulsion and the dispersion can break and flocculate. Therefore, colloids with high zeta potential (negative or positive) are electrically stabilized, while colloids with low zeta potential tend to coagulate or flocculate [11,12].

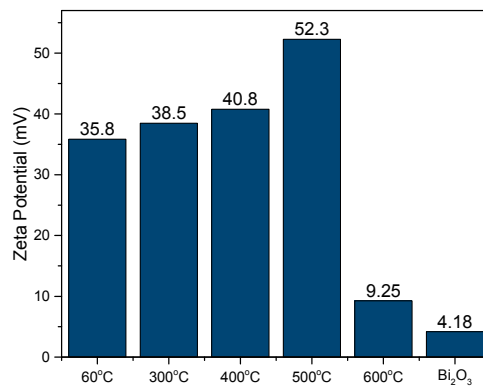


Figure 11. Zeta potential analysis of BiVO₄ microspheres.

3.3. Photocatalytic Properties

Photocatalysis of the samples was evaluated by decolorization of MB aqueous solution under visible light irradiation, and the results are shown in Figures 12 and 13. Absorption of MB aqueous solution at $\lambda = 664 \text{ nm}$ was used to monitor the MB dye decolorization rate process. The decolorization rate sequence can be concluded as 400 °C, 500 °C, 60 °C and 300 °C, followed by 600 °C. Improved performance was observed for 60 °C, 300 °C, 400 °C and 500 °C. However, due to the presence of only agglomeration and bulk structures at 600 °C, the reaction rate declined.

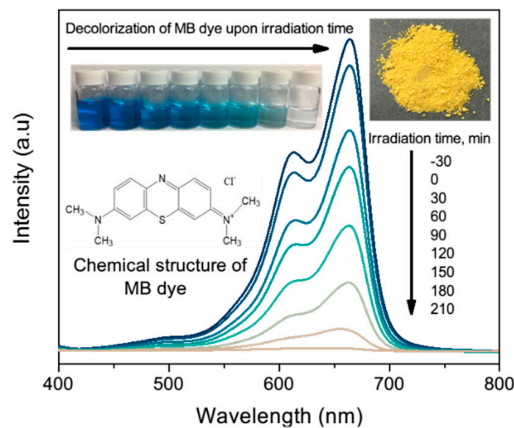


Figure 12. Rate of decolorization of methylene blue dye for BiVO₄ microspheres calcined at 400 °C.

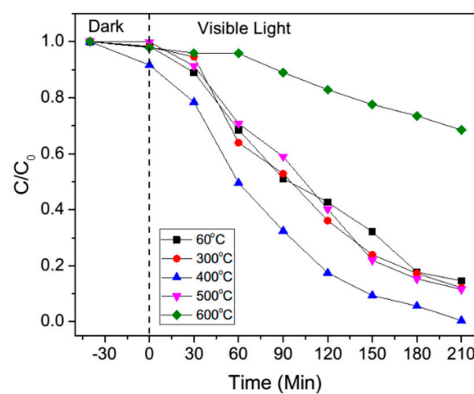


Figure 13. Rate of absorbance of methylene blue dye for BiVO₄ microspheres under calcination temperatures of 60 °C, 300 °C, 400 °C, 500 °C and 600 °C.

In addition, we conducted a Total Organic Carbon (TOC) study (Figure 14) on this photocatalyst, showing that it can degrade MB dye better than commercial BiVO_4 . Thus, it has better efficiency in decolorizing and mineralizing the dye.

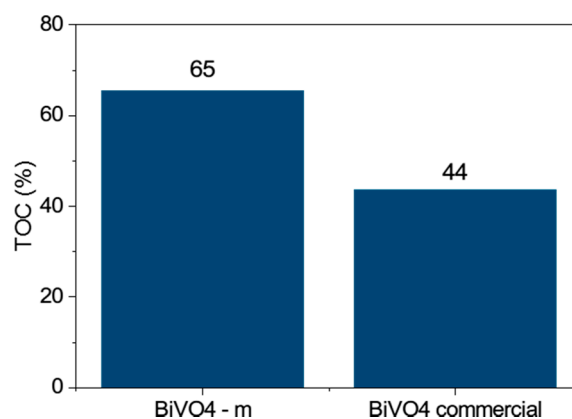


Figure 14. Total Organic Carbon (TOC) percentage of methylene blue dye for BiVO_4 microspheres calcined at $400\text{ }^\circ\text{C}$.

The recyclability of this photocatalyst was also studied (Figure 15). We found that this material has good stability, since it only declined from 94% to 88% after four cycles of the activity, which indicates that it has good stability in this recyclability study.

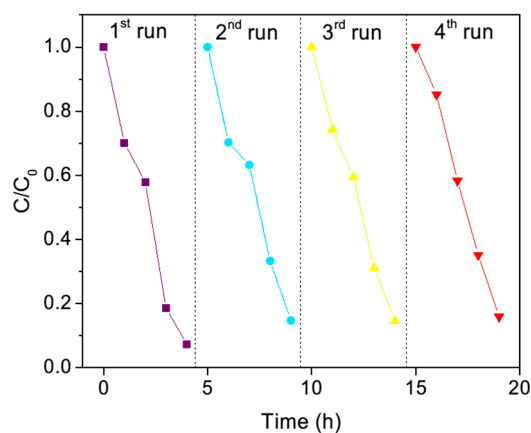


Figure 15. Recyclability of methylene blue dye degradation rate for BiVO_4 microspheres calcined at $400\text{ }^\circ\text{C}$ for four cycles.

4. Conclusions

In conclusion, by adding vanadium (III) acetylacetonate to the system, the flower-like structure can be achieved at a low temperature of $60\text{ }^\circ\text{C}$ for 24 h. Although photocatalysis in decolorization just slightly improved compared to commercial BiVO_4 , it can mineralize the dye better, as can be seen in results of the TOC analysis. We believe that, with further study, the reaction time and photocatalytic performance can be improved. Thus, this work may open the way to possible new and varied low-cost self-assembly synthesizing methods.

Acknowledgments: We are grateful for the acknowledgement support from the National Institute of Material Science.

Author Contributions: Arini Nuran Zulkifili conceived, designed, performed and analyzed the experiments and data; Akira Fujiki and Shinji Kimijima contributed reagents/materials/analysis tools.

Conflicts of Interest: The founding sponsors had no role in the design of the study; in the collection, analysis, or interpretation of data; in the writing of the manuscript; or in the decision to publish the results.

References

1. Fujishima, A.; Honda, K. Electrochemical Photolysis of Water at a Semiconductor Electrode. *Nature* **1972**, *238*, 37–38. [[CrossRef](#)] [[PubMed](#)]
2. Yin, S.; Zhang, Q.; Saito, F.; Sato, T. Preparation of visible light-activated titania photocatalyst by mechanochemical method. *Chem. Lett.* **2003**, *32*, 358–359. [[CrossRef](#)]
3. Zhu, G.; Que, W.; Zhang, J. Synthesis and photocatalytic performance of Ag-loaded β - Bi_2O_3 microspheres under visible light irradiation. *J. Alloys Compd.* **2011**, *509*, 9479–9486. [[CrossRef](#)]
4. Kudo, A.; Omori, K.; Kato, H. A Novel Aqueous Process for Preparation of Crystal Form-Controlled and Highly Crystalline BiVO_4 Powder from Layered Vanadates at Room Temperature and Its Photocatalytic and Photophysical Properties. *J. Am. Chem. Soc.* **1999**, *121*, 11459–11467. [[CrossRef](#)]
5. Zhang, X.; Ai, Z.; Jia, F.; Zhang, L.; Fan, X.; Zou, Z. Selective synthesis and visible light photocatalytic activities of BiVO_4 with different crystalline phases. *Mater. Chem. Phys.* **2007**, *103*, 162–167. [[CrossRef](#)]
6. Shang, M.; Wang, W.; Ren, J.; Sun, S.; Zhang, L. A novel BiVO_4 hierarchical nanostructure: Controllable synthesis, growth mechanism, and application in photocatalysis. *Crystengcomm* **2010**, *12*, 1754–1758. [[CrossRef](#)]
7. Zhou, L.; Wang, W.; Xu, H.; Sun, S.; Shan, M. Bi_2O_3 hierarchical nanostructures: Controllable synthesis, growth mechanism, and their application in photocatalysis. *Chem. Eur. J.* **2009**, *15*, 1776–1782. [[CrossRef](#)] [[PubMed](#)]
8. Meng, X.; Zhang, Z. Bismuth-based photocatalytic semiconductors: Introduction, challenges and possible approaches. *J. Mol. Catal. A Chem.* **2016**, *423*, 533–549. [[CrossRef](#)]
9. Baldan, A. Progress in Ostwald ripening theories and their applications to nickel-base superalloys. *J. Mater. Sci.* **2002**, *37*, 2171–2202. [[CrossRef](#)]
10. Hanaor, D.A.H.; Michelazzi, M.; Leonelli, C.; Sorrell, C.C. The effects of carboxylic acids on the aqueous dispersion and electrophoretic deposition of ZrO_2 . *J. Eur. Ceram. Soc.* **2012**, *32*, 235–244. [[CrossRef](#)]
11. Voorhees, P.W. The theory of Ostwald Ripening. *J. Stat. Phys.* **1985**, *38*, 231–253. [[CrossRef](#)]
12. Greenwood, R.; Kendall, K. Electroacoustic studies of moderately concentrated colloidal suspensions. *J. Eur. Ceram. Soc.* **1999**, *19*, 479–488. [[CrossRef](#)]



© 2018 by the authors. Licensee MDPI, Basel, Switzerland. This article is an open access article distributed under the terms and conditions of the Creative Commons Attribution (CC BY) license (<http://creativecommons.org/licenses/by/4.0/>).